Modifying D-A-π-A-D HTM system for higher hole mobility by the *meta*-substitution strategy to weaken the electron-donating ability of donor unit: A DFT study

Ke-Li Wang [1,§], Qun-Gui Wang [1,§], Cui-E Hu [2,*], Yan Cheng [1,*], Guang-Fu Ji [3], Xiang-Rong Chen[1]

[1] College of Physics, Sichuan University, Chengdu 610064, China;

[2] College of Physics and Electronic Engineering, Chongqing Normal University, Chongqing 400047, China;

[3] National Key Laboratory for Shock Wave and Detonation Physics Research, Institute of Fluid Physics, CAEP, Mianyang 621900, China

Abstract

Tuning the electron-donating ability (EDA) of donor unit of hole transporting materials (HTMs) is an efficient strategy to modulate the optoelectronic properties of HTMs. Based on the strategy, we first theoretically investigated the effects of the EDA of donor unit on the D-A-π-A-D architectural HTMs. Results show that the enhanced EDA of donor unit leads to larger hole reorganization energy and poorer molecular stability of HTM. In contrast, meta-substitution of side-group is an effective strategy to reduce the EDA of donor unit. We found that the application of the meta-substitution strategy in the D-A-π-A-D system not only successfully improves the molecular stability, but also achieves higher hole mobilities by promoting the electronic coupling

* *Corresponding authors. E-mail:* cuiehu@cqnu.edu.cn; ycheng@scu.edu.cn

between the molecular dimers and decreasing the hole reorganization energies simultaneously. Interfacial properties studies indicate the intermolecular coupling also synergistically enhances the interfacial charge extraction performance and reduces the carrier recombination. In conclusion, by utilizing the meta-substitution strategy to reduce the EDA of donor units on D-A-π-A-D architectural HTMs, we successfully designed four superior performance HTMs mD1, mD2, mD3, and mD4.

Keywords: Hole transport materials; Perovskite solar cells; Electron-donating ability; *Meta*-substitution; Hole mobility; Interfacial properties.

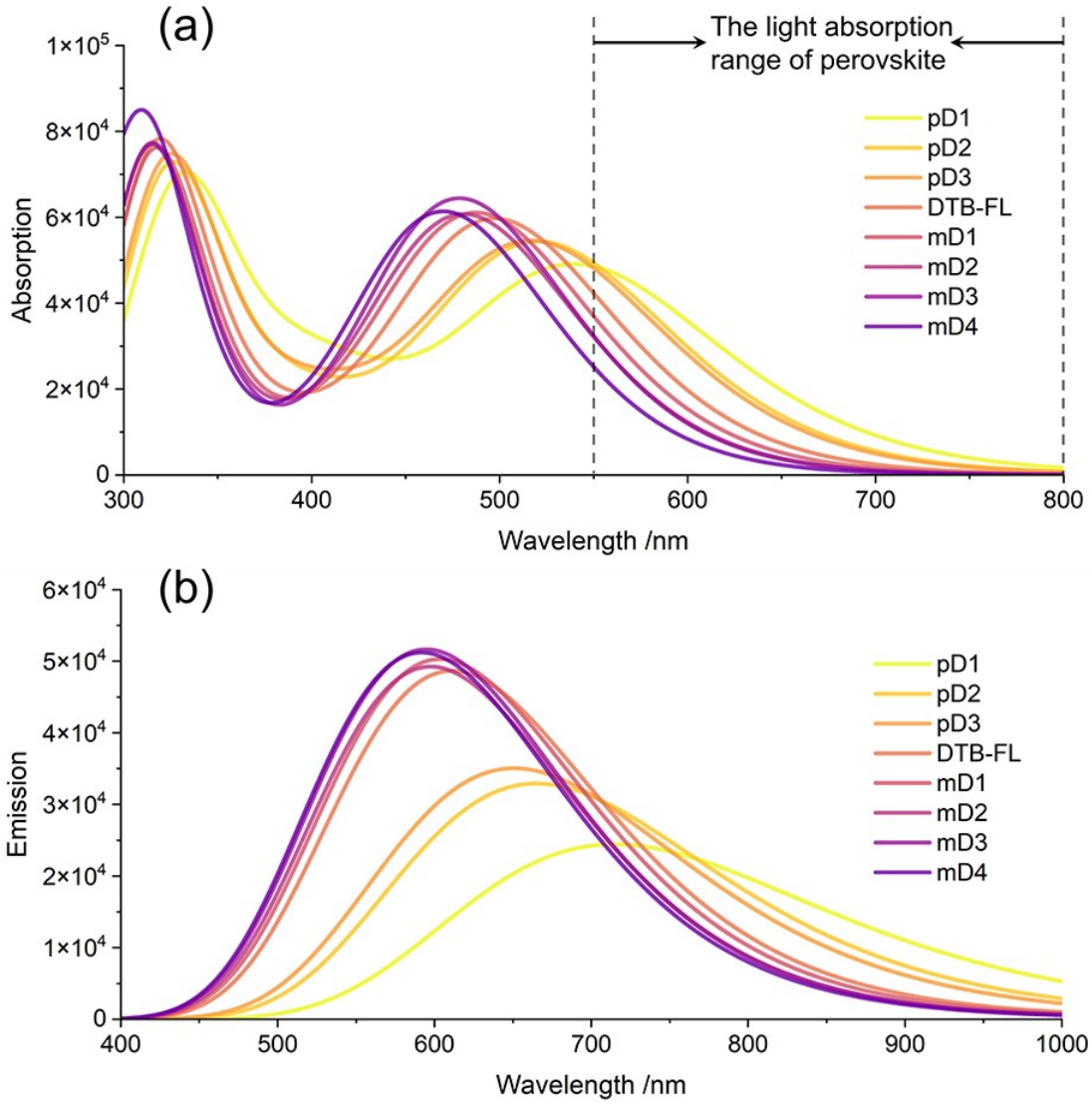

Fig. S1. (Color online) The calculated absorption and emission spectra of eight investigated molecules at the TD-DFT/PBE38/6-31G (d, p) level in dichloromethane.

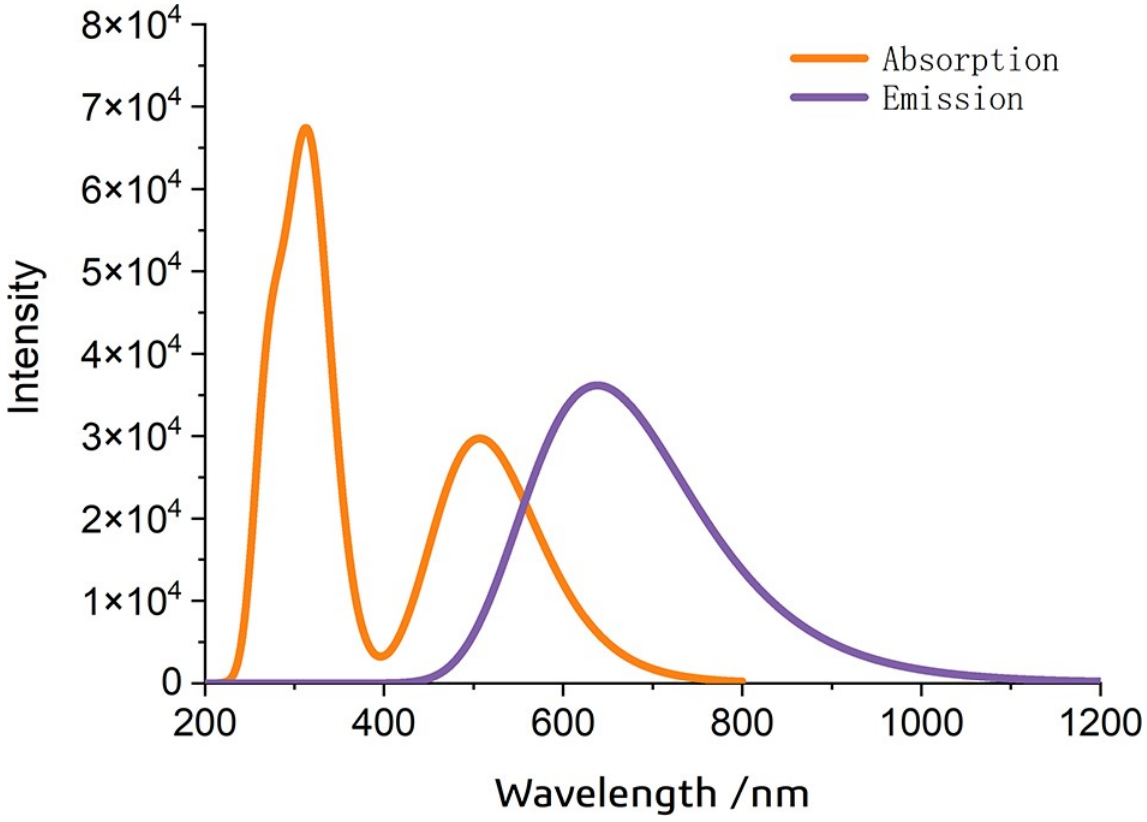

Fig. S2. (Color online) The calculated absorption and emission spectra of DT-BT molecule at the TD-DFT/PBE38/6-31G (d, p) level in dichloromethane.

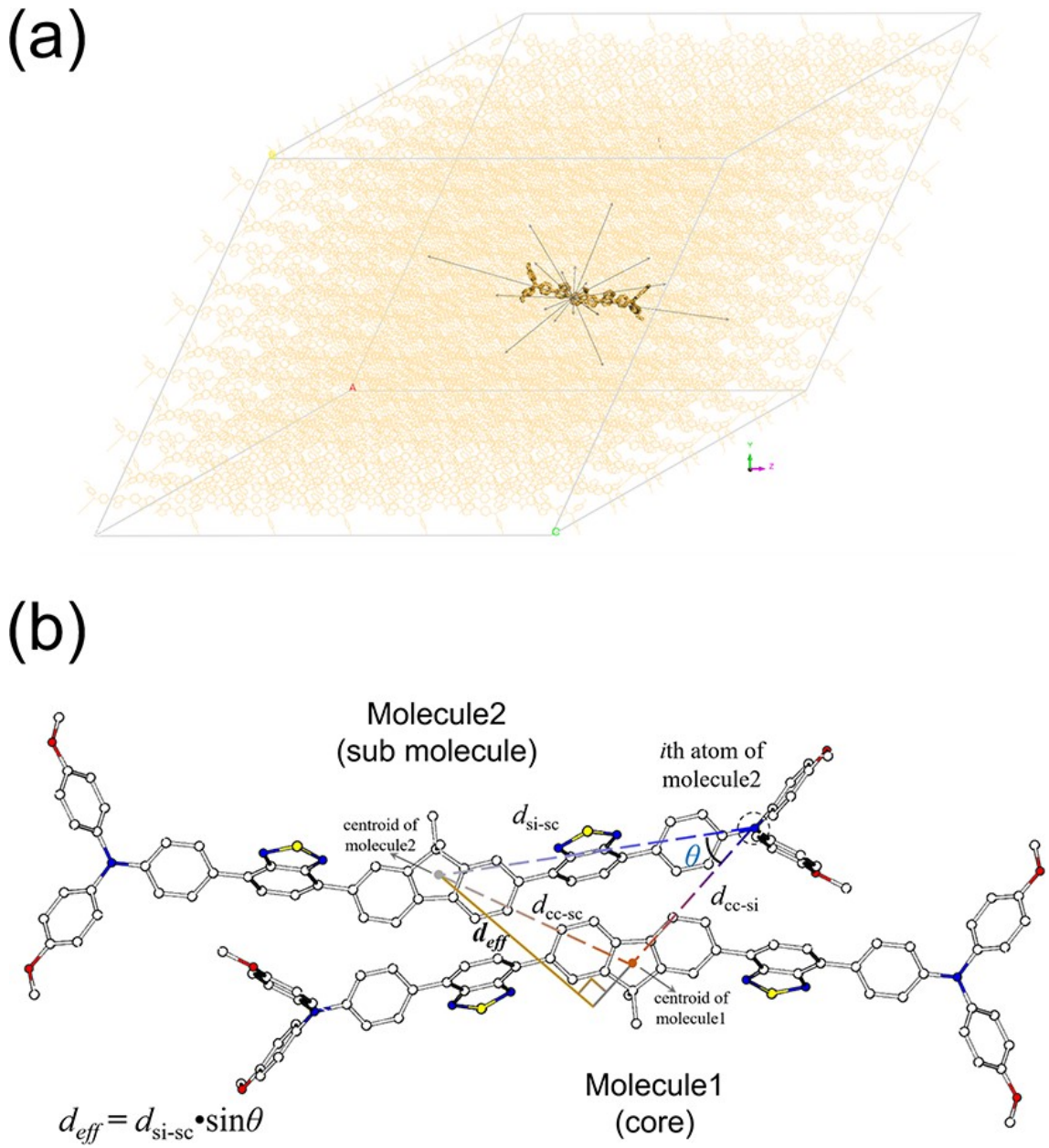

Fig. S3. (Color online) (a). The diagram of giant ideal crystal expanded by the lowest total energy crystal structure; (b). The illustration of the effective distance d_{eff} between molecules of the dimer.

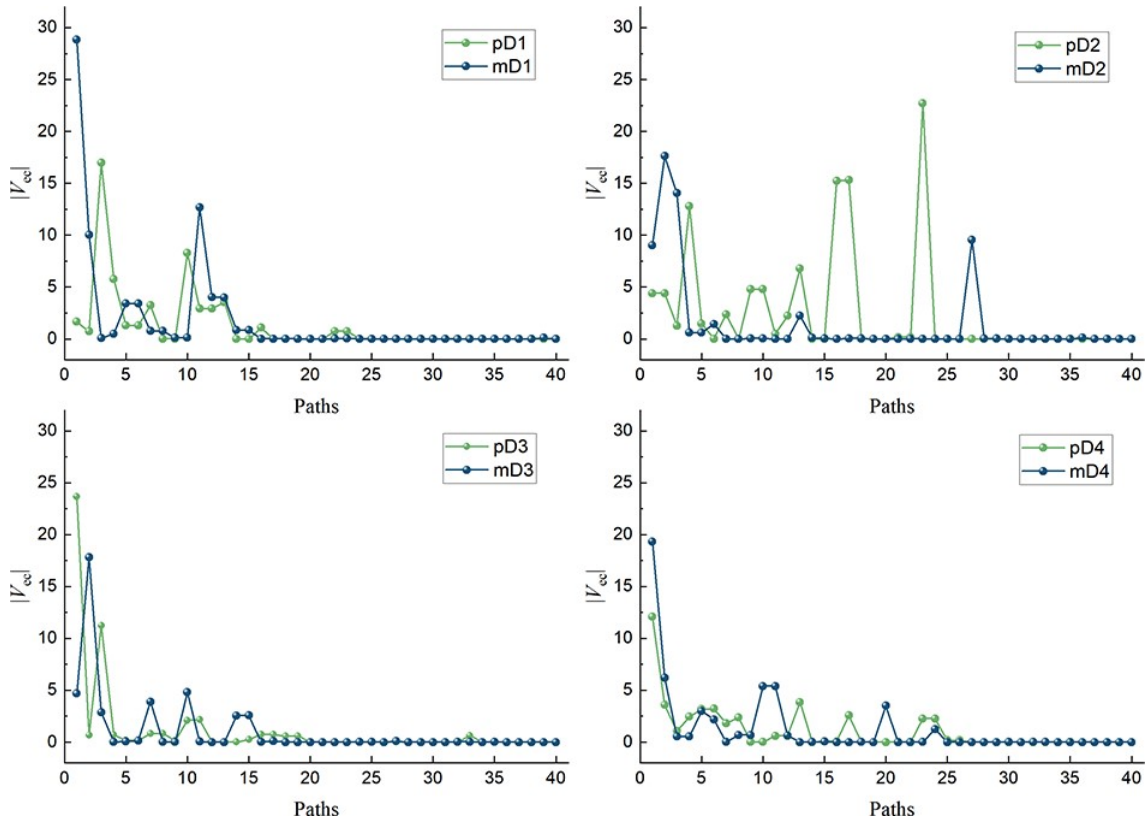

Fig. S4. (Color online) The convergence of electronic coupling of investigated molecules.

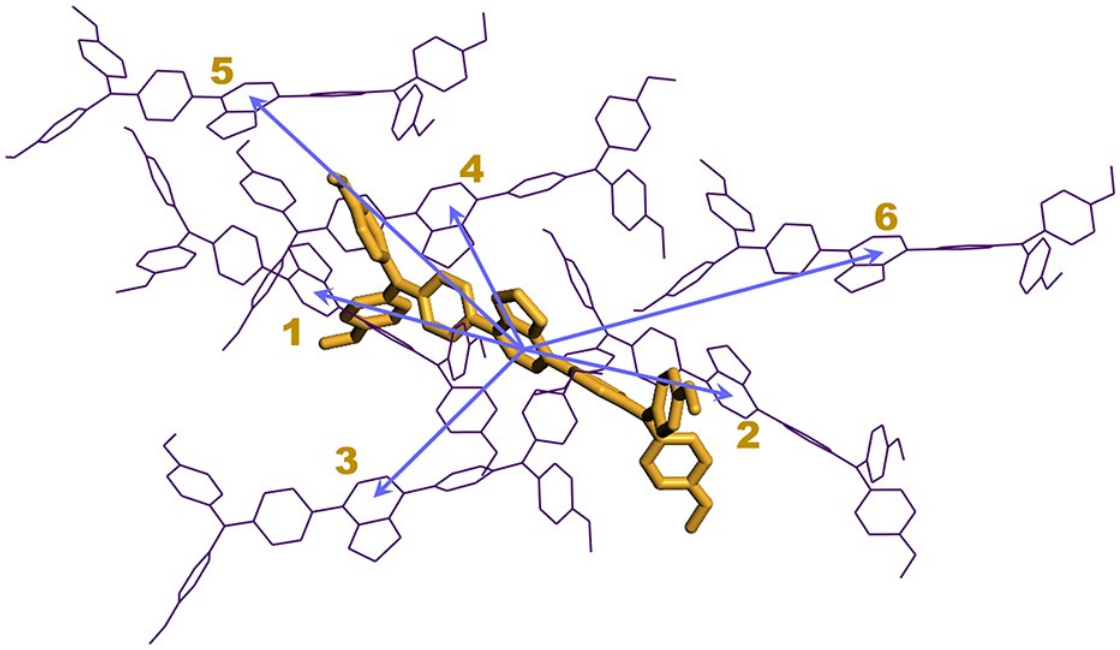

Fig. S5. (Color online) The crystal structure, hopping pathways, and the corresponding hole hopping rate on each main hopping pathway of DT-BT molecules.

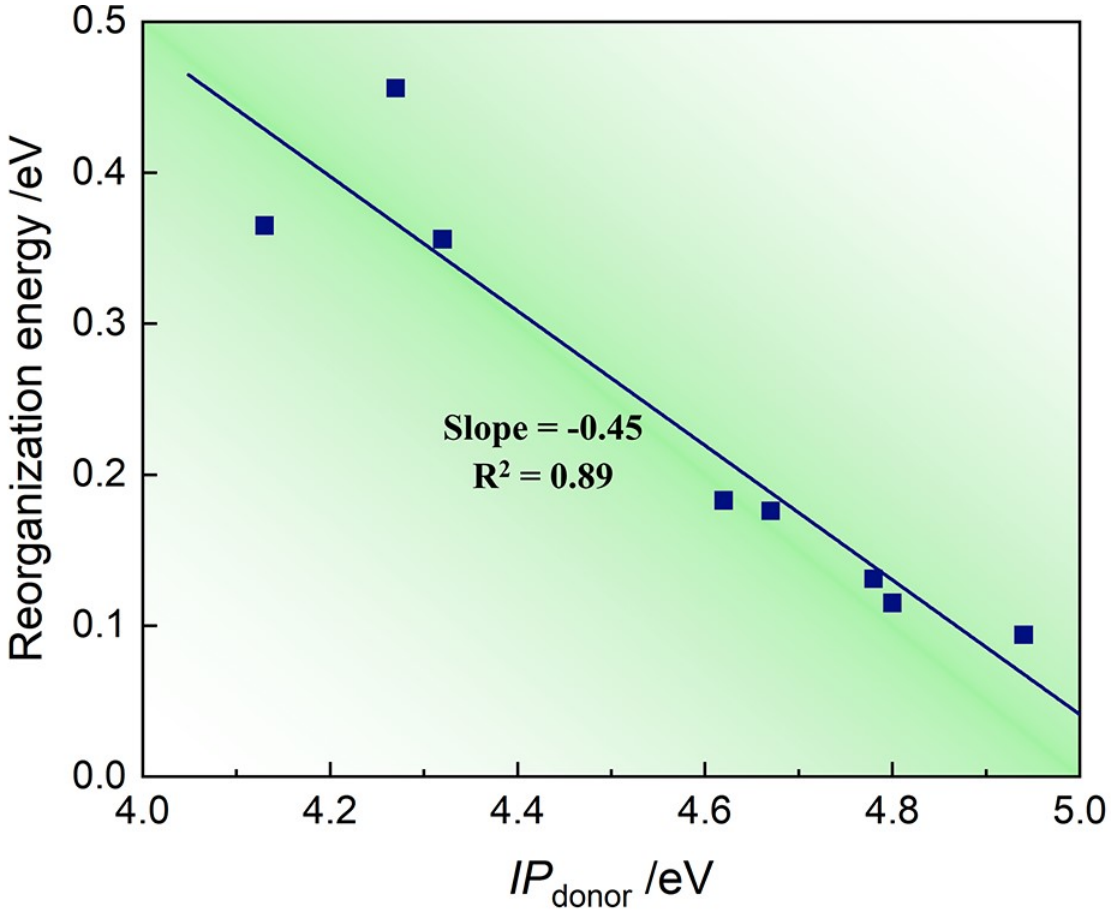

Fig. S6. (Color online) The linear regression fitting of reorganization energy as a function of IP_{donor}.

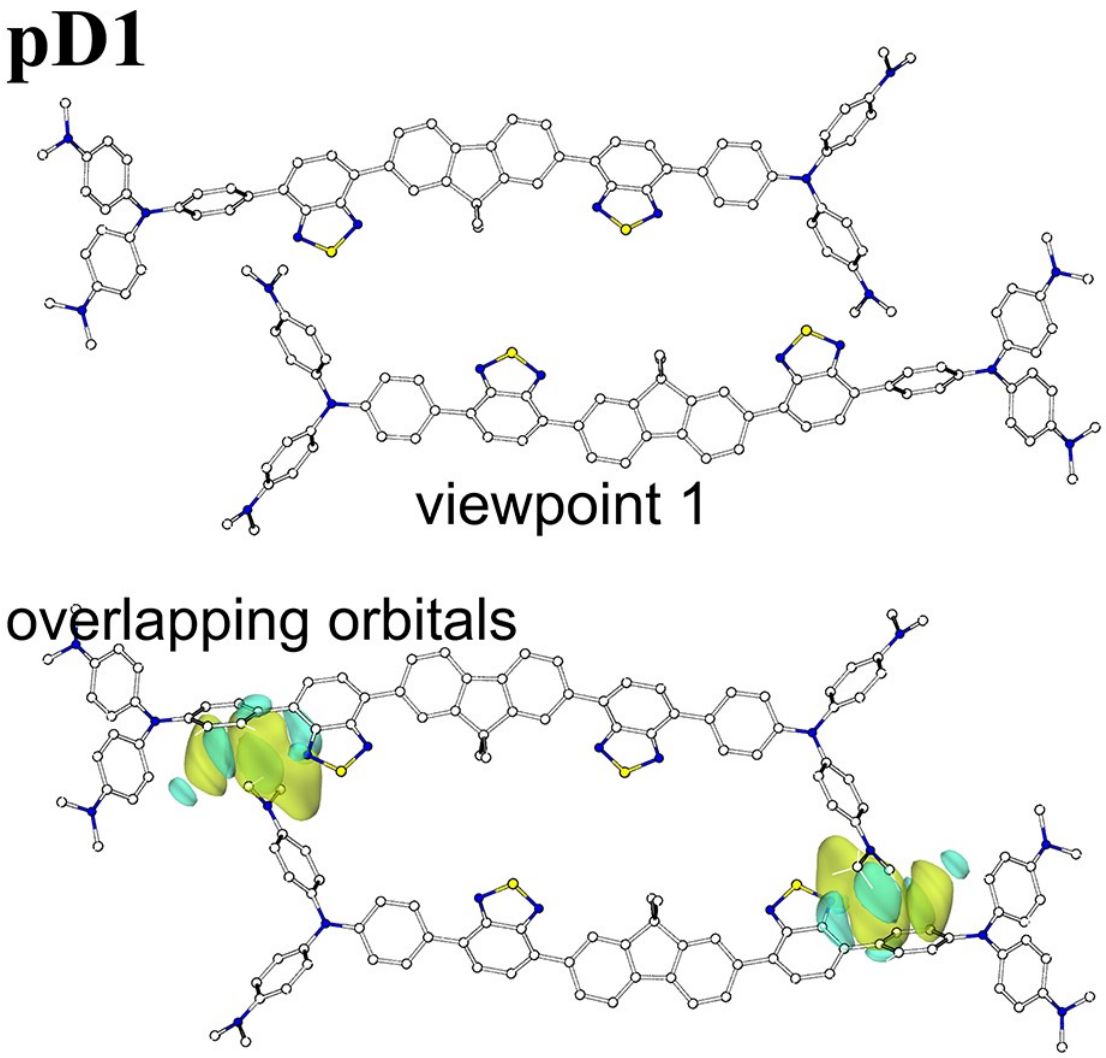

Fig. S7. (Color online) Viewpoint of interacting molecules in the dimer of the predominate hopping path and the overlap between the orbitals of pD1.

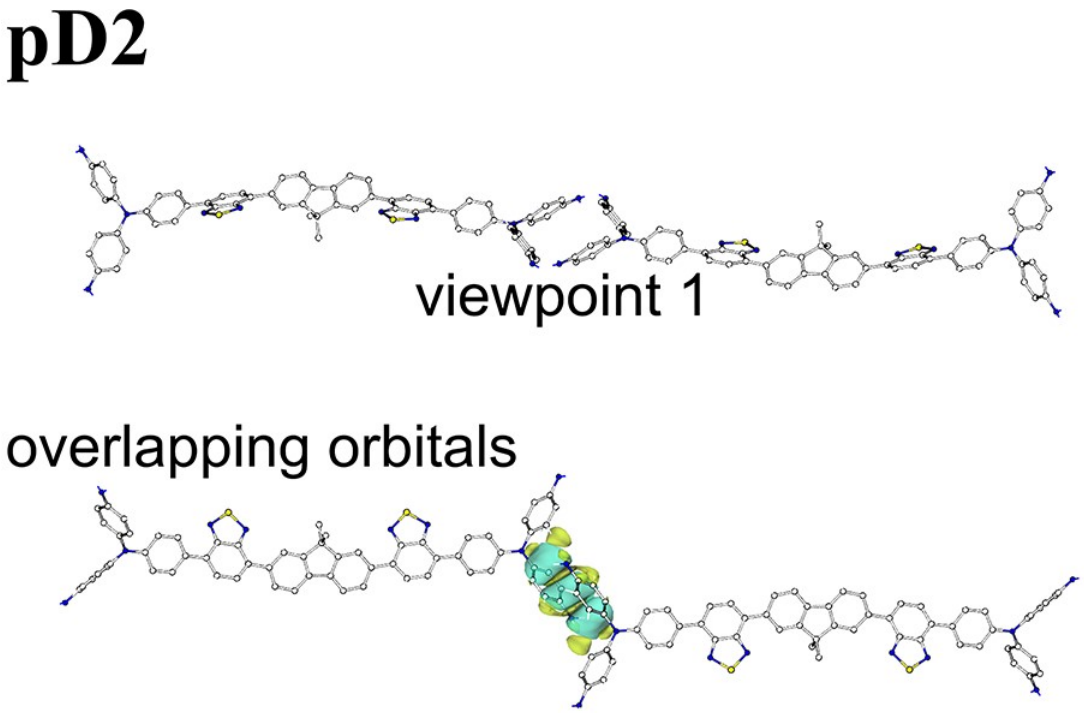

Fig. S8. (Color online) Viewpoint of interacting molecules in the dimer of the predominate hopping path and the overlap between the orbitals of pD2.

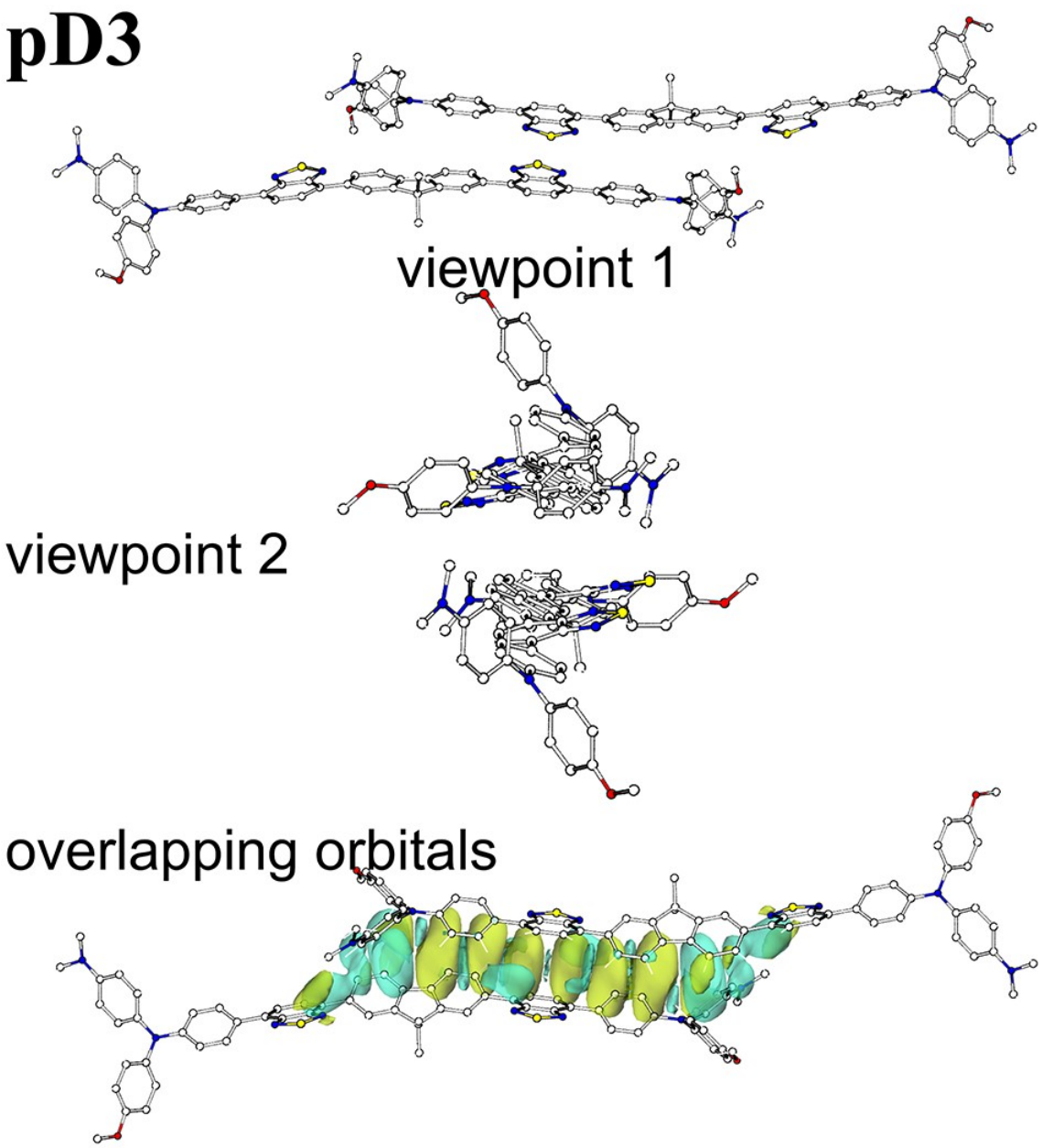

Fig. S9. (Color online) Viewpoints of interacting molecules in the dimer of the predominate hopping path and the overlap between the orbitals of pD3.

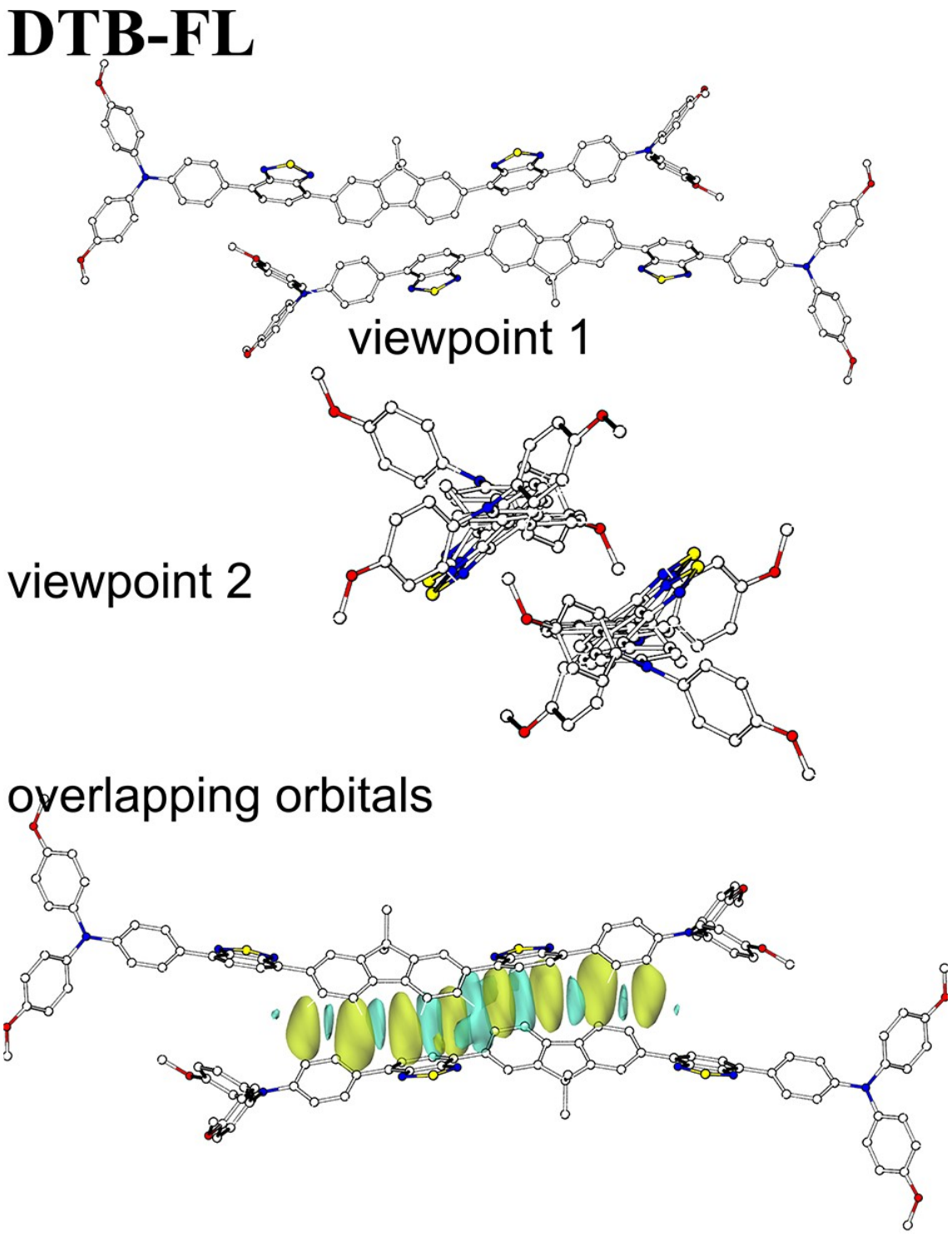

Fig. S10. (Color online) Viewpoints of interacting molecules in the dimer of the predominate hopping path and the overlap between the orbitals of DTB-FL.

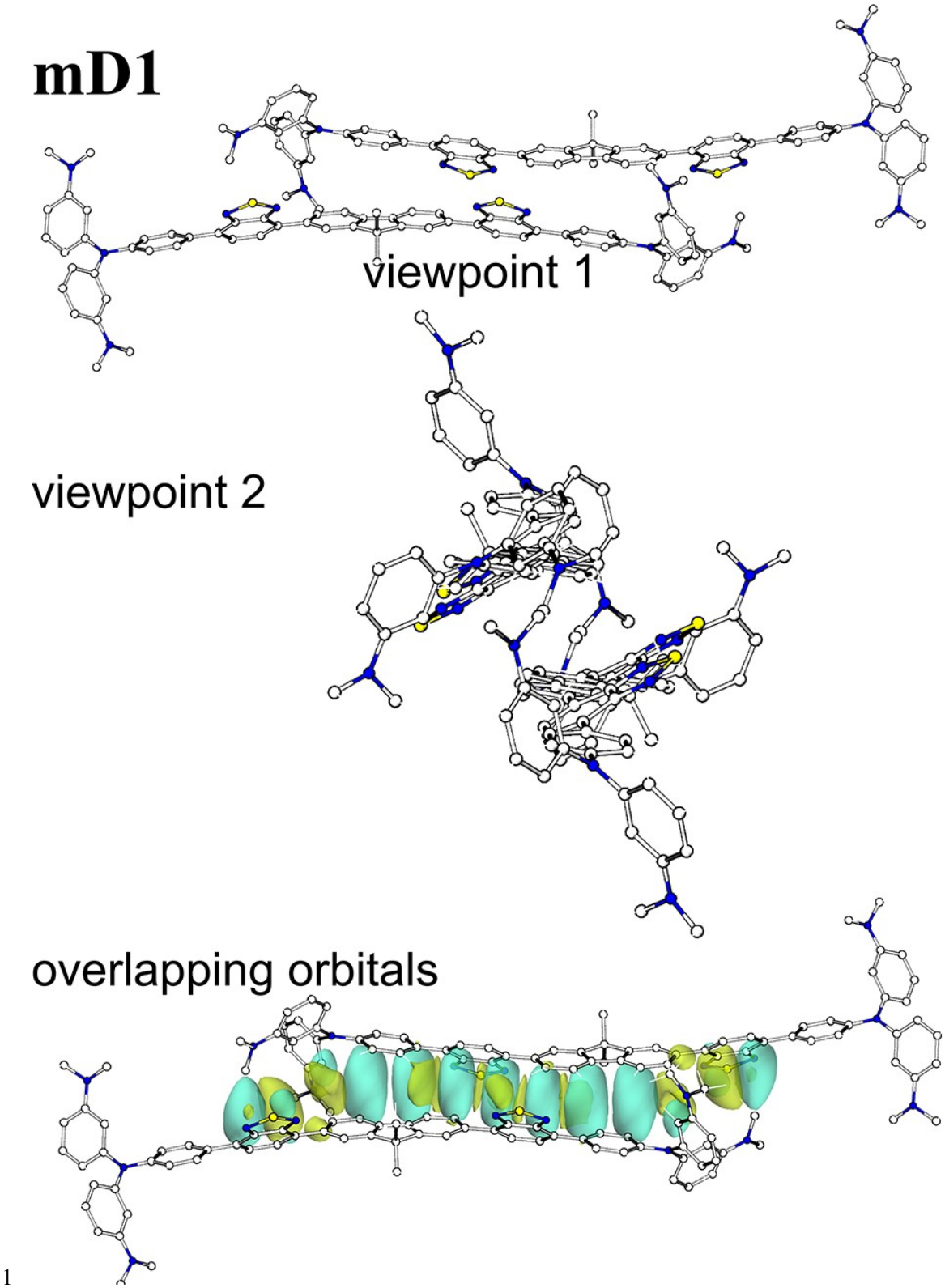

Fig. S11. (Color online) Viewpoints of interacting molecules in the dimer of the predominate hopping path and the overlap between the orbitals of mD1.

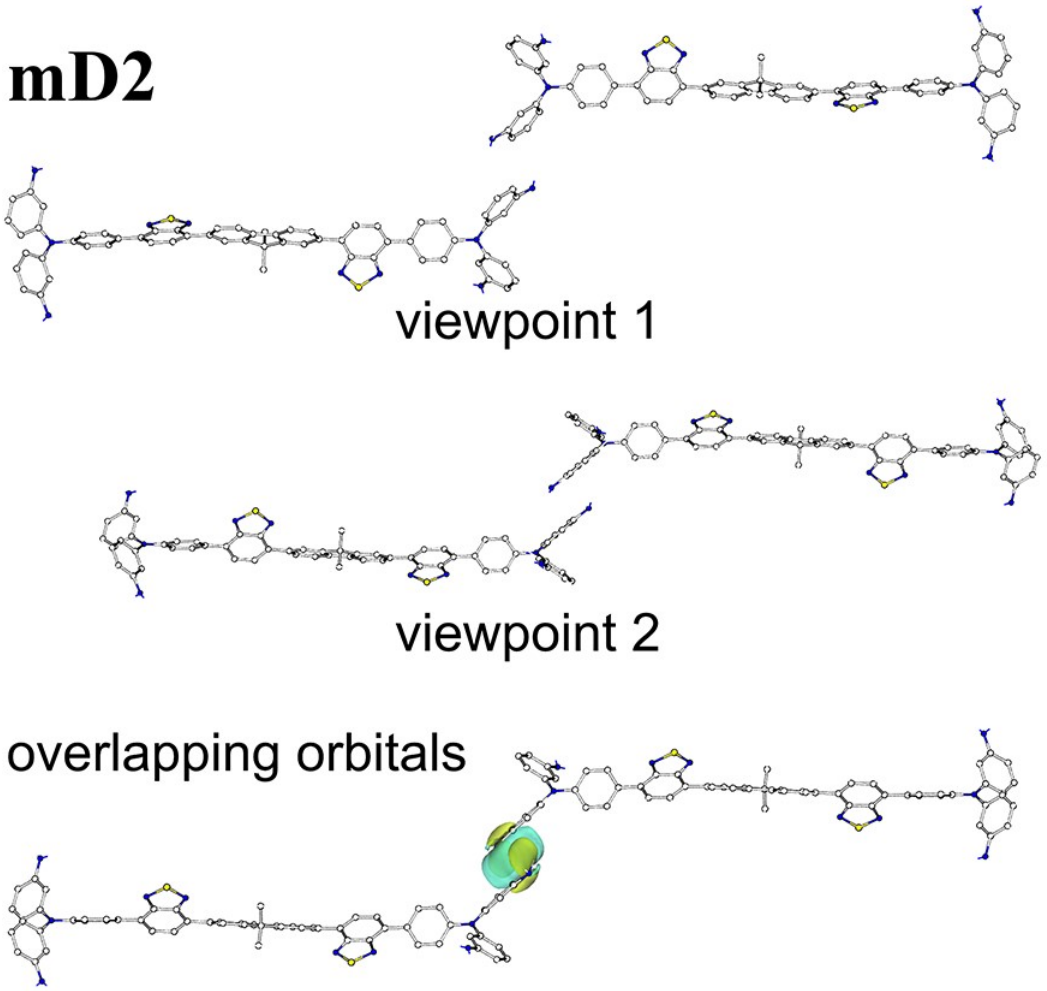

Fig. S12. (Color online) Viewpoints of interacting molecules in the dimer of the predominate hopping path and the overlap between the orbitals of mD2.

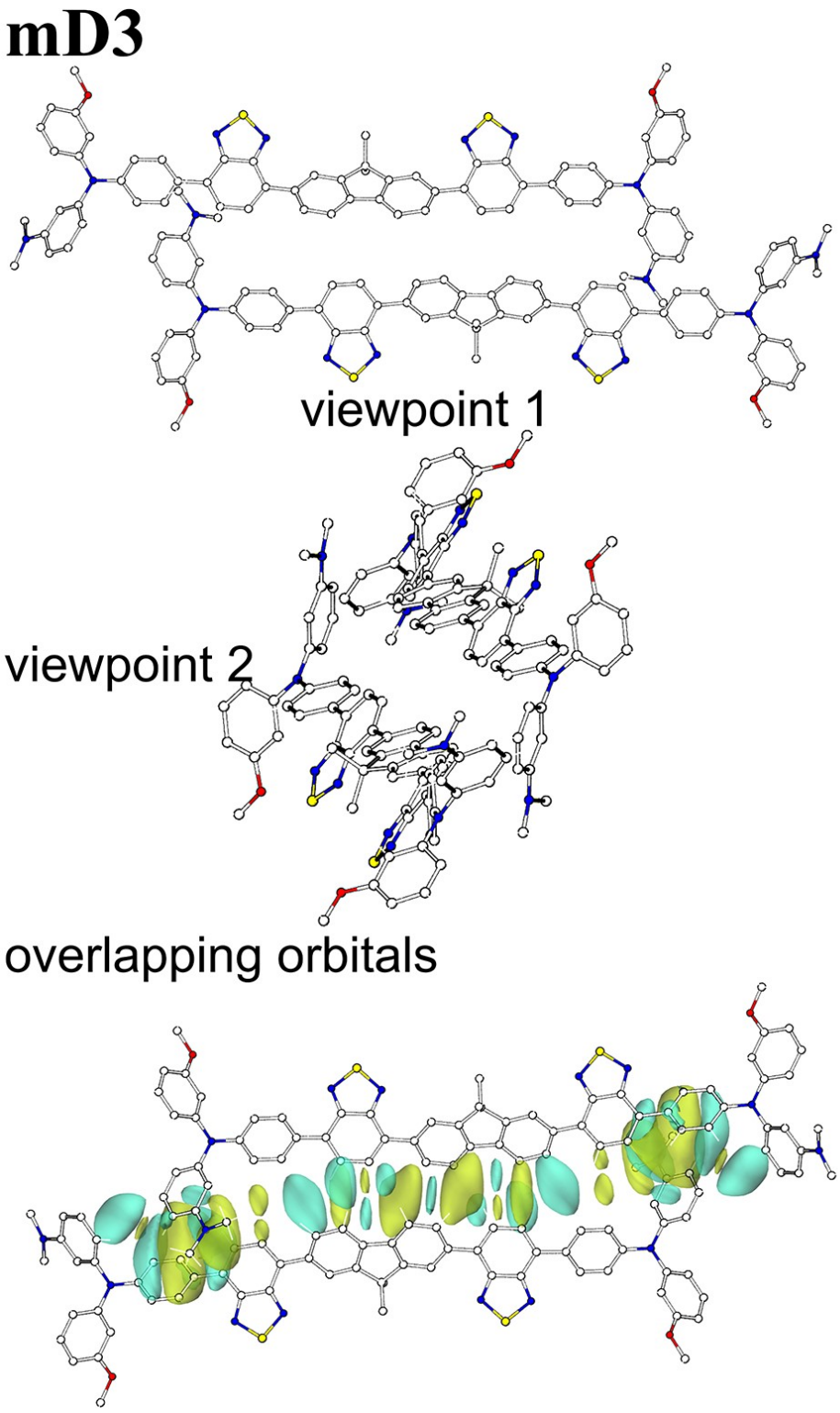

Fig. S13. (Color online) Viewpoints of interacting molecules in the dimer of the predominate hopping path and the overlap between the orbitals of mD3.

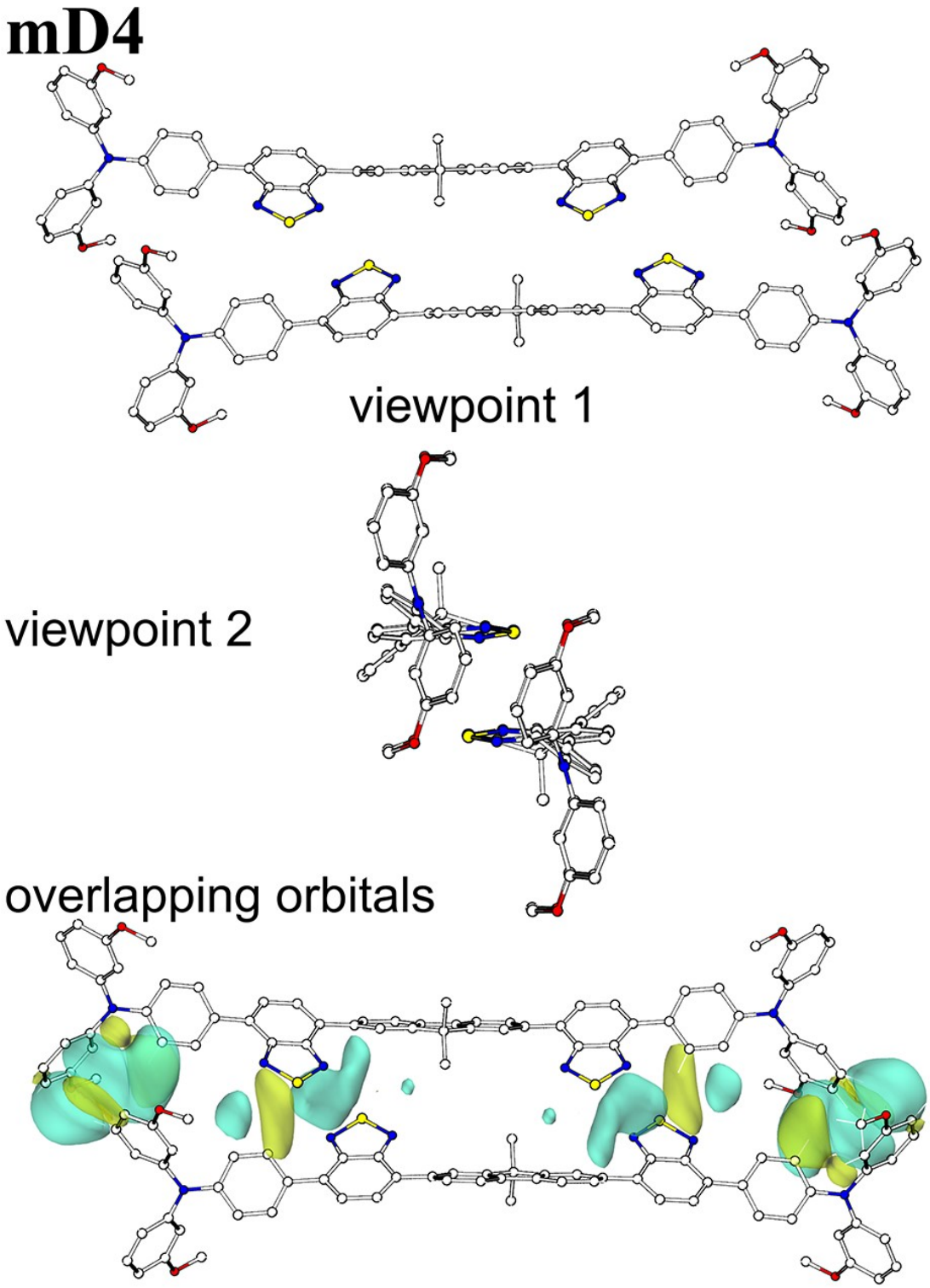

Fig. S14. (Color online) Viewpoints of interacting molecules in the dimer of the predominate hopping path and the overlap between the orbitals of mD4.

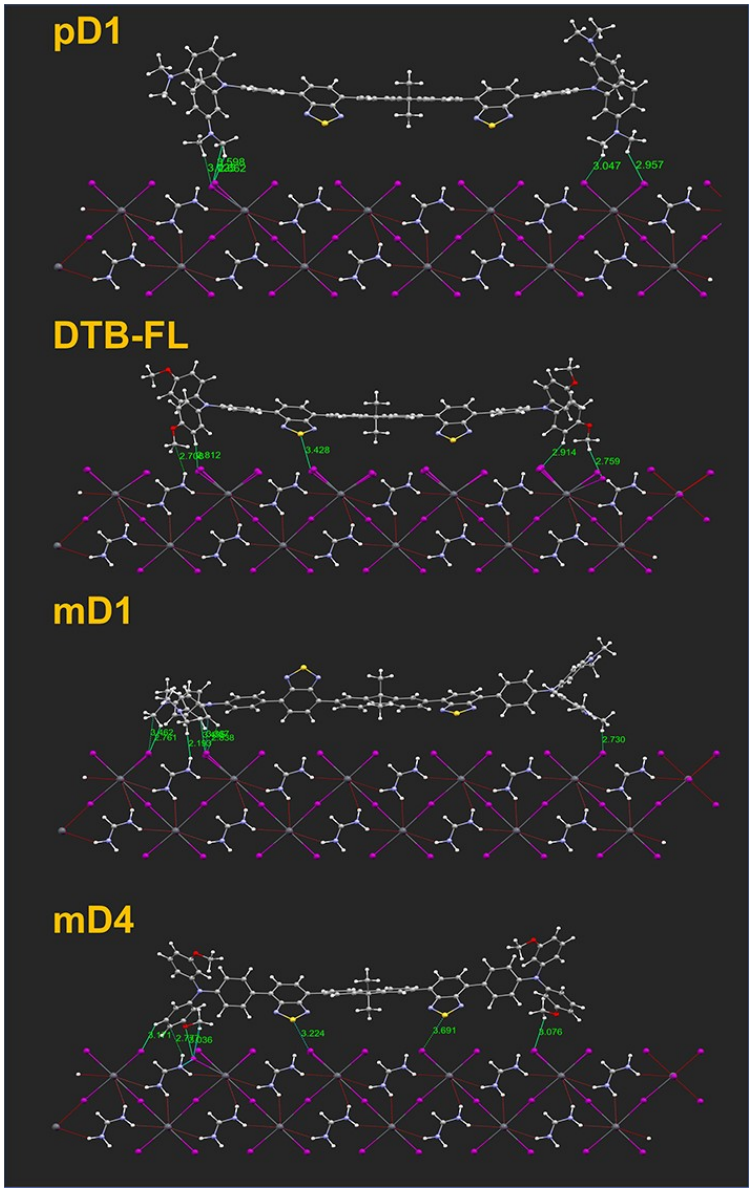

Fig. S15. (Color online) Interfacial interaction between perovskite (110) surface and monomer of pD1, DTB-FL, mD1 and mD4, respectively.

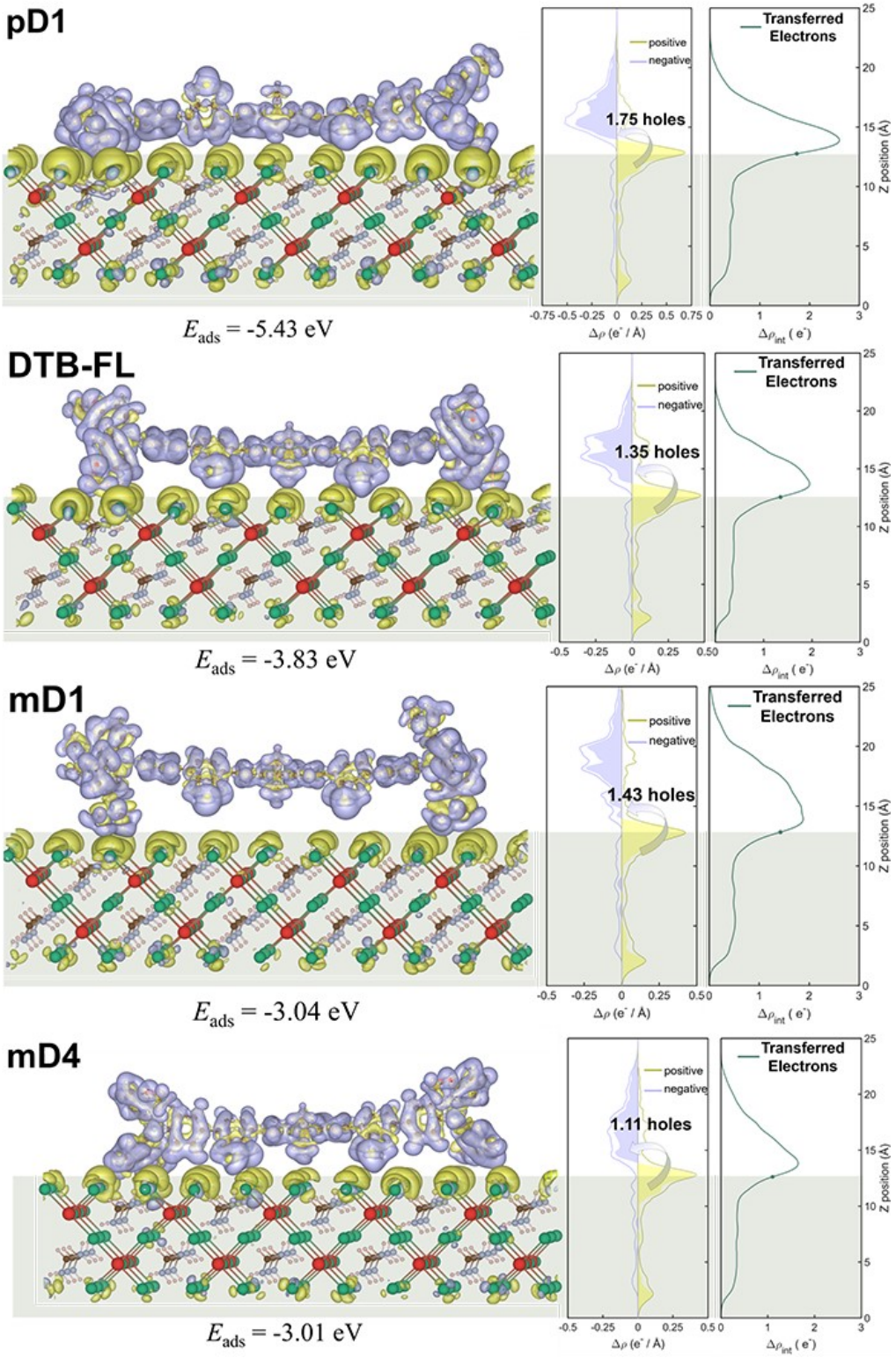

Fig. S16. (Color online) The EDD maps (left), plane-averaged EDD ($\Delta\rho$) of the dimer/perovskite systems integrated in the *x*-*y* plane (central) and the transferred electrons as function of the *z*-axis (right), where light blue and light yellow in EDD

maps and fillings of $\Delta\rho$ diagram represent the accumulation and consumption of electrons, respectively, and the corresponding color curves in $\Delta\rho$ diagram represent the distribution of positive and negative charge carriers.

Fig. S17. The dia

the raw materials

Table S1. The ionization potential and electron affinity of the designed donor unit in the adiabatic condition, are calculated at the B3LYP/6-31G(d, p) level with the PCM model in dichloromethane solvents.

Donor	d1	d2	d3	d4	d5	d6	d7	d8
IP_{donor} /eV	4.13	4.27	4.32	4.62	4.67	4.78	4.80	4.94
EA_{donor} /eV	0.34	0.39	0.43	0.51	0.37	0.42	0.46	0.54

Table S2. The values of HOMO level and LUMO level calculated at B3LYP/6-31G (d, p) level.

Molecules	E_{HOMO} /eV	E_{LUMO} /eV
pD1	-4.43	-2.41
pD2	-4.58	-2.42
pD3	-4.59	-2.43
DTB-FL	-4.78	-2.46
mD1	-4.82	-2.46
mD2	-4.89	-2.48
mD3	-4.90	-2.47
mD4	-5.00	-2.52

Table S3. The fitting values of HOMO and LUMO energy level of investigated molecules by employing the empirical equation proposed by W. J. Chi *et al*. (Ref. 117).

Molecules	E^*_{HOMO} (eV)	E^*_{LUMO} (eV)	E_{Gap} (eV)
pD1	-5.02	-3.00	2.02
pD2	-5.19	-3.03	2.16
pD3	-5.20	-3.04	2.16
DTB-FL	-5.41(-5.47) [a]	-3.09(-3.23) [a]	2.32 (2.24) [a]
mD1	-5.45	-3.09	2.36
mD2	-5.53	-3.12	2.42
mD3	-5.54	-3.11	2.43
mD4	-5.65	-3.16	2.48

[a] Experimental data are obtained from Ref. 53.

Table S4. The calculated and experimental values of HOMO level and LUMO level calculated of DT-BT HTM.

	E^*_{HOMO} /eV	E^*_{LUMO} /eV	E_{Gap} /eV
Calculated	-5.29	-2.95	2.34
Experimental	-5.32	-3.19	2.13

Table S5. The calculated and experimental values of the main absorption peak (λ_{main}) and the absorption peak in the UV-vis region (λ_{abs}) of experimental molecules.

Molecule	DT-BT		DTB-FL	
Absorption type	λ_{main} /nm	λ_{abs} /nm	λ_{main} /nm	λ_{abs} /nm
Computational	317.81	507.09	323.74	499.06
Experimental [a]	314	504	314	492

[a] Experimental data are obtained from Ref. 53.

Table S6. The absorption peak λ_{abs} and emission peak λ_{em}, the excitation energy E and corresponding oscillator strength f_{abs}, the main configuration of investigated molecules, respectively, along with the Stokes shift at the TD-DFT / PBE38 / 6-31G(d, p) level.

Molecules	λ_{abs} (nm)	E	f_{abs}	Main configurations	λ_{em} (nm)	Stokes shifts (nm)
pD1	542.48	2.286	1.185	H→L 56.9% H-1→L+1 27.9%	714.70	172.22
pD2	522.49	2.373	1.310	H→L 61.5% H-1→L+1 27.9%	664.93	142.44
pD3	519.30	2.388	1.310	H→L 60.9%, H-1→L+1 26.8%	650.78	131.48
DTB-FL	499.06 (492) [a]	2.484	1.439	H→L 63.6% H-1→L+1 26.3%	611.28 (805) [a]	112.22
mD1	489.60	2.532	1.463	H→L 59.7% H-1→L+1 23.0%	603.60	114.00
mD2	482.56	2.569	1.470	H→L 63.1% H-1→L+1 24.4%	597.60	115.04
mD3	480.08	2.583	1.556	H→L 61.6% H-1→L+1 21.6%	594.73	114.65
mD4	471.78	2.628	1.478	H→L 64.6% H-→L+1 22.4%	591.87	120.09

[a] The data in bracket are experimental values obtained from Ref. 53.

Table S7. Quantitative analysis of ESPs of the investigated molecules at the isosurface = 0.001 au.

Molecule	Minimal ESP	Maximal ESP	Negative area (%)	Positive area (%)	Negative average ESP	Positive average ESP	Overall average ESP
pD1	-40.85	22.60	59.49	40.51	-12.42	8.73	-3.85
pD2	-39.74	41.15	65.46	34.54	-12.04	11.56	-3.89
pD3	-38.95	23.79	59.60	40.40	-11.41	8.99	-3.17
DTB-FL	-36.29	21.97	57.99	42.01	-10.26	8.72	-2.28
mD1	-36.85	21.71	56.83	43.17	-11.13	7.84	-2.94
mD2	-35.32	39.07	60.59	39.41	-10.78	10.40	-2.43
mD3	-38.15	22.55	58.63	41.37	-11.25	8.47	-3.09
mD4	-31.93	20.57	49.89	50.11	-9.24	8.07	-0.56

Table S8. The crystallographic data of eight HTMs in molecular crystals.

Molecules	Crystal system	Space group	a (Å)	b (Å)	c (Å)	α (°)	β (°)	γ (°)
pD1	Triclinic	P-1	11.949	12.858	43.089	118.454	133.154	87.181
pD2	Triclinic	P-1	29.587	22.575	6.600	84.020	122.647	123.979
pD3	Triclinic	P-1	22.161	20.122	11.630	53.225	65.358	64.959
DTB-FL	Triclinic	P-1	14.988	18.236	20.013	65.195	50.836	50.689
mD1	Triclinic	P-1	12.411	15.337	22.553	81.610	65.732	78.497
mD2	Triclinic	P-1	8.058	37.902	15.466	106.378	124.638	109.169
mD3	Triclinic	P-1	32.849	12.522	10.748	70.973	54.422	87.239
mD4	Triclinic	P-1	25.071	13.325	13.003	92.238	129.053	92.586

Table S9. The reorganization energy λ_h (eV), transfer integral V_{ec} (eV), distance between the centroid to centroid of dimer r (Å), the hole hopping rate k_h (s^{-1}) and the hole mobility μ ($cm^2\ V^{-1}\ s^{-1}$) of DT-BT molecule.

HTMs	Pathway	λ_h	V_{ec}	r	k_h	Contribution	μ
DT-BT	1	0.158	-3.395	9.924	1.05×10^{11}	16.90%	8.348×10^{-3} (1.92×10^{-5}) [a]
	2		-3.391	9.924	1.05×10^{11}	16.82%	
	3		2.018	11.314	3.70×10^{10}	2.74%	
	4		2.016	11.314	3.70×10^{10}	2.73%	
	5		2.948	17.397	7.91×10^{10}	29.52%	
	6		2.95	17.397	7.92×10^{10}	29.60%	

[a] Experimental data are obtained from Ref. 53.

Table S10. The interfacial details of monomer/$FAPbI_3$ and dimer/$FAPbI_3$ heterojunction, including transferred electrons (abbr. as T. E.), Variation of transfer charge between monomer/ $FAPbI_3$ and dimer/ $FAPbI_3$ ($\Delta_{T.E.}$), and interfacial absorption energies (E_{ads}).

	T. E. (monomer/$FAPbI_3$)	T. E. (dimer / $FAPbI_3$)	$\Delta_{T.E.}$	E_{ads} (eV) (monomer/$FAPbI_3$)	E_{ads} (eV) (dimer / $FAPbI_3$)
pD1	1.75	2.23	0.48	-4.56	-5.43
DTB-FL	1.35	2.06	0.71	-3.48	-3.83
mD1	1.43	1.99	0.56	-3.34	-3.04
mD4	1.11	1.80	0.70	-2.82	-3.01